IVYSPRING INTERNATIONAL PUBLISHER

Theranostics

2018; 8(19): 5348-5361. doi: 10.7150/thno.27385

Research Paper

# Prostaglandin $E_2$ hydrogel improves cutaneous wound healing via M2 macrophages polarization

Shuaiqiang Zhang[1, 2], Yuanyuan Liu[3], Xin Zhang[1], Dashuai Zhu[1], Xin Qi[4], Xiaocang Cao[3], Yihu Fang[5, 6, 7], Yongzhe Che[1], Zhong-Chao Han[8], Zuo-Xiang He[9], Zhibo Han[7,10]✉, Zongjin Li[1, 2, 11]✉

1. Nankai University School of Medicine, Tianjin, China;
2. The Key Laboratory of Bioactive Materials, Ministry of Education, Nankai University, the College of Life Science, Tianjin, China;
3. Department of Hepato-Gastroenterology, Tianjin Medical University General Hospital, Tianjin Medical University, Tianjin, China;
4. Department of Cardiology, Tianjin Union Medical Center, Nankai University Affiliated Hospital, Tianjin, China;
5. JiangXi Medical College, Shangrao, Jiangxi, China;
6. Jiangxi Engineering Research Center for Stem Cell, Shangrao, Jiangxi, China;
7. National Engineering Research Center of Cell Products, AmCellGene Co., Ltd., Tianjin China;
8. Beijing Engineering Laboratory of Perinatal Stem Cells, Beijing Institute of Health and Stem Cells, Health & Biotech Co., Beijing, China;
9. Department of Nuclear Medicine, Beijing Tsinghua Changgung Hospital, Tsinghua University, Beijing, China;
10. State Key Lab of Experimental Hematology, Chinese Academy of Medical Sciences & Peking Union Medical College, Tianjin, China;
11. State Key Laboratory of Kidney Diseases, Chinese PLA General Hospital, Beijing, China.

✉ Corresponding authors: Zongjin Li, MD, PhD, School of Medicine, Nankai University, 94 Weijin Road, Tianjin 300071, China, Ph: +86-22-23509332, Fax: +86-22-23509505, Email: zongjinli@nankai.edu.cn; or Zhibo Han, State Key Lab of Experimental Hematology, Chinese Academy of Medical Sciences & Peking Union Medical, 288 Nanjing Road, Tianjin 300020, China. Ph: +86-22-23909999, Fax: +86-022-23909999, E-mail: zhibohan@163.com



Received: 2018.05.21; Accepted: 2018.09.28; Published: 2018.10.22

## Abstract

Wound healing is regulated by a complex series of events and overlapping phases. A delicate balance of cytokines and mediators in tissue repair is required for optimal therapy in clinical applications. Molecular imaging technologies, with their versatility in monitoring cellular and molecular events in living organisms, offer tangible options to better guide tissue repair by regulating the balance of cytokines and mediators at injured sites.

**Methods:** A murine cutaneous wound healing model was developed to investigate if incorporation of prostaglandin $E_2$ ($PGE_2$) into chitosan (CS) hydrogel (CS+$PGE_2$ hydrogel) could enhance its therapeutic effects. Bioluminescence imaging (BLI) was used to noninvasively monitor the inflammation and angiogenesis processes at injured sites during wound healing. We also investigated the M1 and M2 paradigm of macrophage activation during wound healing.

**Results:** CS hydrogel could prolong the release of $PGE_2$, thereby improving its tissue repair and regeneration capabilities. Molecular imaging results showed that the prolonged release of $PGE_2$ could ameliorate inflammation by promoting the M2 phenotypic transformation of macrophages. Also, CS+$PGE_2$ hydrogel could augment angiogenesis at the injured sites during the early phase of tissue repair, as revealed by BLI. Furthermore, our results demonstrated that CS+$PGE_2$ hydrogel could regulate the balance among the three overlapping phases—inflammation, regeneration (angiogenesis), and remodeling (fibrosis)—during cutaneous wound healing.

**Conclusion:** Our findings highlight the potential of the CS+$PGE_2$ hydrogel as a novel therapeutic strategy for promoting tissue regeneration via M2 macrophage polarization. Moreover, molecular imaging provides a platform for monitoring cellular and molecular events in real-time during tissue repair and facilitates the discovery of optimal therapeutics for injury repair by regulating the balance of cytokines and mediators at injured sites.

Key words: prostaglandin $E_2$ ($PGE_2$), macrophages, molecular imaging, hydrogel, wound healing, angiogenesis

## Introduction

Tissue repair and regeneration following injury, surgery or in diseases remains a significant clinical challenge [1, 2]. In response to tissue damage, complex biological processes are involved in the

activation and coordination of numerous cellular and molecular pathways [3]. Effective tissue repair and regeneration proceed in sequential phases of inflammation, tissue formation, and remodeling involving a complex orchestration of resident stem cells, immune cells, cytokines, and extracellular matrix (ECM) [4]. However, imbalances or defects in these processes can perturb the delicate equilibrium of cells and signaling pathways necessary for complete tissue repair, which can result in chronic wounds and fibrotic scars, further impairing normal tissue functions and ultimately leading to organ failure and death [4, 5]. Ideally, the aim for tissue repair in the clinic is to achieve an optimal balance between cytokines and mediators; however, the field has not yet produced therapeutically applicable outcomes [4].

Recent studies revealed that tissue repair and regeneration are orchestrated by immune responses to tissue damage in the local microenvironment including networks of cellular and signaling components [1, 4]. Macrophages are considered the primary effector cells in regulating tissue repair and the reprogramming of macrophage phenotype is mediated through the microenvironment of injured sites [6-11]. Rapid advances in stem cell therapy have demonstrated that prostaglandin $E_2$ ($PGE_2$) secreted by mesenchymal stem cells (MSCs) might induce M2 phenotype of macrophages to attenuate sepsis [12] and promote cutaneous wound healing [13]. These findings suggest that $PGE_2$ not only can relieve inflammation but also has significant therapeutic potential for tissue regeneration through macrophages.

$PGE_2$, a lipid-signaling molecule that acts as both an inflammatory mediator and a fibroblast modulator, is a promising therapeutic candidate for improving tissue repair and regeneration [14, 15]. Moreover, suppression of $PGE_2$ inhibits tissue regeneration and leads to excessive wound scar formation [16, 17]. However, the short half-life of $PGE_2$ in circulation results in less contact time with cells and hampers the ability of $PGE_2$ to effectively participate in physiological processes [18]. Engineered bio-matrices can provide temporally and spatially controlled release of growth factors or cytokines, providing the possibility to mimic the complex signaling patterns of endogenous tissue regeneration [1, 19, 20]. Furthermore, designed biomimetic scaffolds can recruit native stem cells to sites of injury and stimulate the body's own healing mechanisms [1, 4].

In this study, we hypothesized that chitosan (CS) hydrogel incorporating $PGE_2$ (CS+$PGE_2$ hydrogel) could prolong the release of $PGE_2$ and might have a better effect on tissue repair and regeneration. To test this hypothesis, we assessed the therapeutic effects of CS+$PGE_2$ hydrogel in a murine model of cutaneous wound healing. We investigated the kinetic regulation of macrophage polarization by CS+$PGE_2$ hydrogel both *in vivo* and *in vitro*. Furthermore, by using molecular imaging approaches, we monitored CS+$PGE_2$ hydrogel-derived anti-inflammatory and pro-angiogenesis responses in wound healing.

## Methods

### Preparation of CS+$PGE_2$ hydrogel

CS hydrogel was prepared as previously reported [19]. Ultra-pure CS (M=200000; Haidebei Bioengineering Company, Jinan, China) with a deacetylation degree of 90% was used to prepare the gel. In brief, 200 mg CS was dissolved in 20 mL HCl (0.1 M) stirred overnight, dialyzed through a membrane (molecular cut-off of 8 kDa to 10 kDa) using 2 L of distilled water for 1 week to ensure removal of residual acetic acid and then lyophilized to obtain CS hydrochloride. CS hydrochloride (2% w/v) solution was prepared in β-glycerophosphate (β-GP) (70% w/v) (Sigma Aldrich, Ireland) in sterile water. The ice-cold β-GP solution (2.29 M) was added to the CS solution dropwise with stirring in an ice bath for about 0.5 h. CS hydrogel was stored at 0-8 ℃. The pH value of the dialyzed CS/β-GP solution was 7.2. The preparation process of chitosan hydrogel incorporating $PGE_2$ (CS+$PGE_2$ hydrogel) was as described above except that $PGE_2$ (Santa Cruz Biotechnology, Santa Cruz, CA) solution was added dropwise to the CS solution while stirring on ice for 30 min. A homogenous gel was obtained by adding the β-GP solution to the chitosan/$PGE_2$ solution dropwise while stirring on ice. The final concentrations of CS and β-GP in the mixture were 1.9% w/v and 0.68% w/v, respectively. The $PGE_2$ powder was dissolved in phosphate buffered saline (PBS) or water to prepare the $PGE_2$ solution without hydrogel at a concentration of 0.1 mg/mL to 5 mg/mL.

### Harvesting of macrophages

Peritoneal macrophages were harvested as previously reported [21]. In brief, 3 days after intraperitoneal injection of 3 mL 3% thioglycolate solution (Sigma-Aldrich, St. Louis, MO), the mice were anesthetized with 4% chloral hydrate. The cell suspensions containing the vast majority of macrophages (about 95%) were collected by peritoneal lavage. The harvested cells were cultured in 6-well flat-bottom culture plates at a density of $3\times10^6$ cells per well with Dulbecco's Modified Eagle's Medium (DMEM; Gibco, Grand Island, NY) and 3% fetal bovine serum (FBS; HyClone, Australia). After incubation for 2-4 h, the nonadherent cells were

removed by rinsing with PBS. To investigate if peritoneal macrophages could be stimulated by lipopolysaccharides (LPS), the cells were treated with interleukin-4 (IL-4; 20 ng/mL) (Sigma Aldrich, St Louis, Mo), LPS (10 ng/mL) (Sigma Aldrich, St Louis, Mo), free $PGE_2$ (1 μM) or $PGE_2$ hydrogel (1 μM) for 48h.

### Enzyme-linked immunosorbent assay

To investigate if CS hydrogel could prolong the halftime of $PGE_2$ in culture system, $2\times10^5$ peritoneal macrophages per well were seeded in 24 well-plates. Free $PGE_2$ or CS+$PGE_2$ hydrogel was added to the culture medium with an equal amount of $PGE_2$ (1 ng per well) in each experimental system. The supernatants were collected at indicated times over 48 h. The concentration of $PGE_2$ in culture mediums was measured by commercially available ELISA kits (Cayman Chemicals, Ann Arbor, MI) according to the manufacturer's protocol.

### CCK-8 assay

To investigate if $PGE_2$ could affect the proliferation of macrophages, the mouse peritoneal macrophages were seeded into 96-well plates at a density of $1\times10^4$ cells per well with different concentrations of $PGE_2$ (0.5 μM, 1 μM, 1.5 μM and 2 μM). After incubating for 24 h and 48 h, the reagent of Cell Counting Kit-8 (CCK-8; Dojindo Molecular Technologies, Rockville, MD) was added to the medium and incubated for an additional 2 h. The absorbance value of each well was recorded at 450 nm using a microplate reader (Thermo Labsystems, Vantaa, Finland).

To determine if the stability of CS+$PGE_2$ hydrogel is affected by the storage temperature, a cell proliferation assay was performed. Mouse peritoneal macrophages were seeded into 96-well plates at a density of $1\times10^4$ cells per well and CS+$PGE_2$ hydrogel stored at different temperature conditions (-80 ℃, 0 ℃, 4 ℃ and 37 ℃) was added to the 96-well plate with a final $PGE_2$ concentration of 1 μM. Cell proliferation was analyzed after 24 h by using a CCK-8 Kit.

### Skin wound healing model

*VEGFR2-Luc* transgenic mice (Xenogen Corp, Hopkinton, MA) constitutively expressing firefly luciferase (Fluc) under the promoter of vascular endothelial growth factor receptor 2 (*VEGFR2-luc*) [19, 22], was used in this study. Mice were raised under a specific pathogen-free (SPF) animal area at Animal Facility of Nankai University. Protocols were approved by the Animal Ethical Committee of the Nankai University Animal Care and Use Committee Guidelines, which conform to the Guide for the Care and Use of Laboratory Animals published by the US National Institutes of Health (8th Edition, 2011). The mice were anesthetized with intraperitoneal injection of chloral hydrate (4%, 350 mg/kg). Wounds were created using sterile ophthalmic scissors with a diameter of 1 cm skin full-thickness in the back deep to the fascia. A silicone film 0.5 mm in thickness was sutured on the wound to prevent wound contraction [23]. All mice were randomly divided into 4 groups, and the sites of injury of each group were evenly smeared with 20 μL of PBS, CS, $PGE_2$ (10 μM) and CS+$PGE_2$ hydrogel (10 μM) (n=10 of each group). To determine the efficacy of multiple applications of the CS+$PGE_2$ hydrogel, we performed extra experiments. Mice received single $PGE_2$ hydrogel (CS+$PGE_2$ hydrogel was only administered on day 0 after injury for treatment), double (days 0 and 2), or triple (days 0, 2 and 4) treatments. The wound area was measured using ImageJ software (NIH, Bethesda, MD) by a blinded researcher at various time points (0, 1, 4, 7, 10, and 14 days). To ensure the accuracy of the data, the 10 wounds were measured at each time point for each treatment group and the experiments were performed in triplicate. The percent of original wound area was calculated as follows: wound area (%) = (wound area on day n/wound area on day 0) × 100 (%).

### Histology analysis

At day 7 and 14 after injury, the mice were euthanized, and skin samples were harvested and fixed. Hematoxylin-Eosin (H&E) and Masson's staining were performed to detect wound healing and collagen deposition at the injured sites. Immunofluorescence staining was carried out to determine the angiogenic and macrophage effects at different time points. To detect angiogenic effects, rat anti-mouse CD31 (*Abcam*, *Cambridge*, *MA*) and Alexa Fluor 594 goat anti-rat IgG (Invitrogen, Grand Island, NY) were used. To track macrophages, anti-F4/80 (Abcam, Cambridge, UK), anti-CD68 (Abcam), anti-RELM-α (Abcam), anti-CD206 (Abcam), and anti-iNOS antibodies (Abcam) were used. Moreover, anti-α-SMA antibody (Boster Bio-Engineering Company, Wuhan, China) was used to evaluate infiltration of myofibroblasts at the injured sites. Alexa Fluor 488 and 594 (Invitrogen, Carlsbad, CA) were applied appropriately. The cell nuclei were counter-stained with 4', 6-diamidino-2-phenylindole (DAPI). Immunohistochemistry was performed to detect the expression of interleukin-1β (IL-1β) (Boster Bio-Engineering Company, Wuhan, China). The images were analyzed by ImageJ software.

### Bioluminescence imaging

To monitor the angiogenic effects of the CS+$PGE_2$ hydrogel *in vivo*, bioluminescence imaging

(BLI) of the *VEGFR2-Luc* mice was performed using IVIS Lumina II system (Xenogen Corporation, Hopkinton, MA) as previously described [19, 22, 24]. The anesthetized mice were intraperitoneally injected with firefly luciferase substrate D-Luciferin (150 mg/kg; Biosynth International, Naperville, IL) to evaluate the expression of VEGF-R2. Furthermore, to detect the reactive oxygen species (ROS) at the injured site, the mice were injected with luminol (10 mg/kg; Sigma Aldrich Chemie, Steinheim, Germany). The mice were imaged with the IVIS Lumina II system 5 min after injection of the substrate. Bioluminescence signals were quantified in units of maximum photons per second per centimeter squared per steradian (photons/s/cm$^2$/sr) as described [22, 25].

### Western blot analysis

Cells were lysed on ice in radio-immunoprecipitation assay (RIPA) buffer. For tissue proteins analysis, the mouse skin tissue was cut in a 1.5 mL EP tube supplemented with a proteinase inhibitor cocktail (Sigma) and transferred to a homogenizer. The tissue homogenates were lysed on ice with RIPA for 30 min. Harvested proteins were separated on 10% SDS-PAGE and transferred to polyvinylidene fluoride membranes (PVDF; Millipore, Darmstadt, Germany). The primary antibodies included β-actin (1:1000, Santa Cruz Biotechnology, CA), collagen I (1:300, Boster Bio-Engineering Company, Wuhan, China), IL-10 (1:1000, Abcam, Cambridge, UK) and IL-6 (1:1000, Abcam, Cambridge, UK). β-actin was used as an internal control.

### Quantitative real-time PCR

Total RNA was isolated from cells or tissues using TRIzol reagent (Invitrogen, Grand Island, NY) and was purified using RNeasy columns (Qiagen, Chatsworth, CA). First-strand cDNA was synthesized by reverse transcriptase (TransGen Biotech, China) using oligo dT primers. Subsequently, TransStart Green qPCR SuperMix Kit (TransGen Biotech, China) was used to quantify the mRNA expression levels in 20 μL reaction volumes. Real-time PCR analysis was performed on the Opticon® System (Bio-Rad, Hercules, CA). The $2^{-\Delta\Delta Ct}$ method was used to analyze relative gene expression. The sequences of primers are listed in **Table S1**.

### Statistical analysis

Statistical analysis was performed using GraphPad Prism 5.0 software (GraphPad Software Inc., San Diego, CA). Statistically significant differences between groups were assessed by ANOVA or two-tailed Student's *t*-test. Differences were considered significant at $P$ values < 0.05.

## Results

### Characterization of CS+PGE$_2$ hydrogel

Scanning electron microscopy (SEM) analysis showed that CS+PGE$_2$ hydrogel was homogeneous and had interconnected pores with an average pore size of about 50 μm (**Figure 1A**). The CS+PGE$_2$ hydrogel was thermosensitive and could transform from liquid at room temperature to hydrogel at 37 °C (**Figure 1B**). CCK-8 assay revealed that PGE$_2$ could promote proliferation of macrophages at an optimal concentration of 1 μM (**Figure 1C**). To investigate whether the CS hydrogel could prolong the half-life of PGE$_2$ in the culture system, the supernatants were analyzed by ELISA. The results showed that the concentration of PGE$_2$ in the culture medium increased continually, reaching a peak at 10 h, then decreased over a period of 48 h, whereas the concentration of PGE$_2$ decreased sharply without the CS hydrogel (**Figure 1D**). To test the stability of CS+PGE$_2$ hydrogel, peritoneal macrophages were cultured with CS+PGE$_2$ hydrogel stored at different temperatures for 7 days. Cell proliferation assay revealed that the stability of PGE$_2$ hydrogel was not influenced by the storage conditions (**Figure 1E**).

### CS+PGE$_2$ hydrogel augments skin regeneration

To assess the therapeutic efficacy of the CS+PGE$_2$ hydrogel *in vivo*, a murine model of cutaneous wound healing was used. For this purpose, the injured sites were treated with CS+PGE$_2$ hydrogel, PGE$_2$, or CS and the areas of the wound were measured every 3 days. Compared with other groups (PGE$_2$, CS, and PBS), CS+PGE$_2$ hydrogel promoted wound contraction and accelerated the wound healing processes (**Figures 2A-C**). Furthermore, CS+PGE$_2$ hydrogel treatment demonstrated a more regenerative healing with improved skin structures including a greater return of hair follicles and sebaceous glands on day 14 (**Figure S1A-B**). To observe the efficacy of multiple applications of the CS+PGE$_2$ hydrogel, skin tissues were harvested on day 14 after treatment. HE staining revealed that multiple dosing of PGE$_2$ could lead to tissue hyperplasia and extra scar formation (**Figure S2**).

### Enhanced anti-inflammatory and angiogenic effects of CS+PGE$_2$ hydrogel *in vitro*

Recent studies have demonstrated that PGE$_2$ could induce macrophage polarization to M2 phenotype *in vitro* [12]. To investigate whether CS+PGE$_2$ hydrogel could reinforce its ability of phenotype transformation, we cultured macrophages with PBS, CS, PGE$_2$ and CS+PGE$_2$ hydrogel for 48 h.

CD68 and CD206, which are highly expressed in M2 phenotype macrophages, were significantly increased when the cells were co-cultured with CS+$PGE_2$ hydrogel (**Figure S3A-C**). These results were consistent with the expression of M2 macrophage-related genes (IL-10, IL-1RA and Arg-1) after CS+$PGE_2$ hydrogel treatment for 48 h (**Figure 3A**). Additionally, CS+$PGE_2$ hydrogel repressed the expression of M1 phenotype macrophages-related genes (IL-6, TNF-α, IL-1β) after treatment for 48 h (**Figure 3B**). The expression of M2 phenotype macrophages-related IL-10 and M1 phenotype macrophage-related IL-6 were analyzed by Western blotting. The results demonstrated that CS+$PGE_2$ hydrogel could promote the expression of IL-10 but inhibit the expression of IL-6 (**Figure S4A-B**). Also, RT-PCR results showed that, compared with other groups (LPS, CS and $PGE_2$), CS+$PGE_2$ hydrogel could significantly up-regulate the expression of CD206 (M2 phenotype macrophage) but inhibit the expression of iNOS (M1 phenotype macrophage) (**Figure S3D**). These findings indicated that CS+$PGE_2$ hydrogel could promote M2 macrophage polarization even in an inflammatory microenvironment.

To gain insight into the mechanisms of CS+$PGE_2$ hydrogel-induced early angiogenesis, we cultured macrophages with CS, $PGE_2$, and CS+$PGE_2$ hydrogel for 48 h *in vitro* followed by RT-PCR analysis. Our results revealed that angiogenesis-related genes VEGF-A, PLGF, b-FGF, Ang-2, Ang-1, and PDGF-BB were significantly upregulated in the CS+$PGE_2$ hydrogel-treated group compared with other groups (**Figure 3C**). These findings suggest that CS+$PGE_2$ hydrogel might induce the proangiogenic effects of macrophages and further promote cutaneous angiogenesis after injury.

## Enhanced anti-inflammatory effects of CS+$PGE_2$ hydrogel *in vivo*

Inflammatory infiltration occurs early in the repair of wounds and plays a key role in injury repair [26]. To evaluate the effect of CS+$PGE_2$ hydrogel on inflammatory response of the injured sites, inflammatory infiltration of a mouse skin wound model was monitored by BLI in real time [27]. Inflammatory tissues can generate reactive oxygen species (ROS) [13], including many different types of molecular oxygen, which could be detected with luminol through BLI technology [28]. By analyzing the BLI signals of all groups from day 1 to 10, we observed that the ROS levels in the groups treated with CS+$PGE_2$ hydrogel and $PGE_2$ decreased from day 4, whereas the ROS levels of PBS and CS groups decreased from day 7 (**Figure 4A-B**). It has been reported that M1 macrophages are abundant during the early inflammatory response and produce a high amount of ROS and pro-inflammatory cytokines. We next analyzed the number of M1 macrophages at the injury sites on day 4 after skin injury. Compared with other groups, CS+$PGE_2$ hydrogel significantly decreased the accumulation of M1 macrophages (**Figure 4C**). Furthermore, CS+$PGE_2$ hydrogel also significantly reduced the local levels of pro-inflammatory cytokines IL-1β on day 4 after injury (**Figure 4D**). These results indicated that CS+$PGE_2$ hydrogel could decrease infiltration of inflammatory cells by an anti-inflammatory effect at the injured sites through a time-dependent regulation of ROS. CS+$PGE_2$ hydrogel also accelerated cutaneous wound healing, at least in part, by inhibiting infiltration of inflammatory cells and secretion of pro-inflammatory cytokines at injured sites.

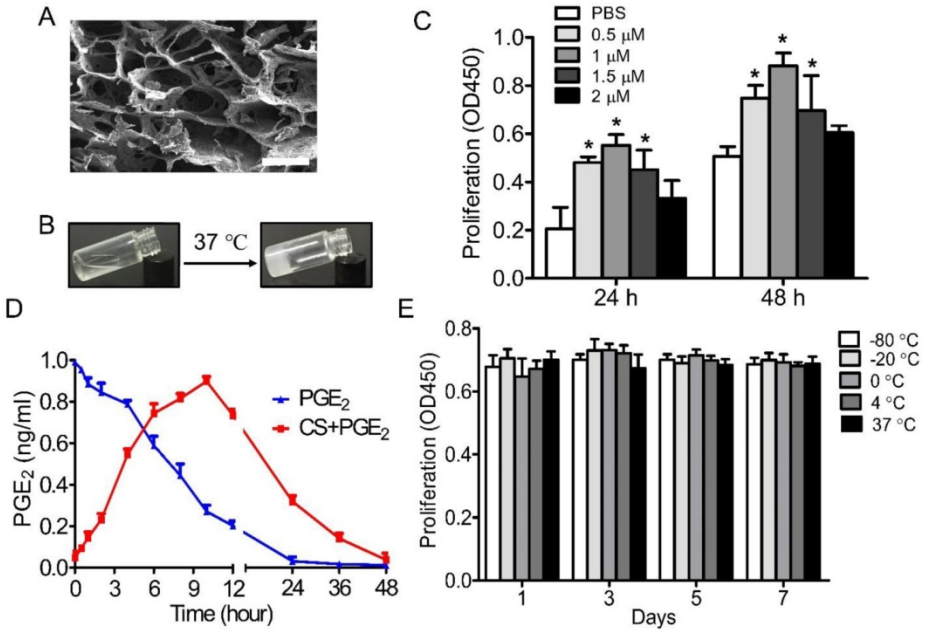


**Figure 1. Characterization of CS+$PGE_2$ hydrogel. (A)** Scanning electron microscopy (SEM) morphology of CS+$PGE_2$ hydrogel. Scale bars, 100 μm. **(B)** CS+$PGE_2$ solution formed a hydrogel at 37 °C. **(C)** CCK-8 assay showed proliferation of macrophages with different concentrations of $PGE_2$. **(D)** Release profile of $PGE_2$ in the presence or absence of CS hydrogel by ELISA. **(E)** Cell proliferation of macrophages treated with CS+$PGE_2$ hydrogel stored under different temperature conditions up to 7 days. Data are expressed as mean ± SD. *$P$ < 0.05 versus PBS. All experiments were performed in triplicate. CS+$PGE_2$: CS+$PGE_2$ hydrogel; $PGE_2$: free $PGE_2$.

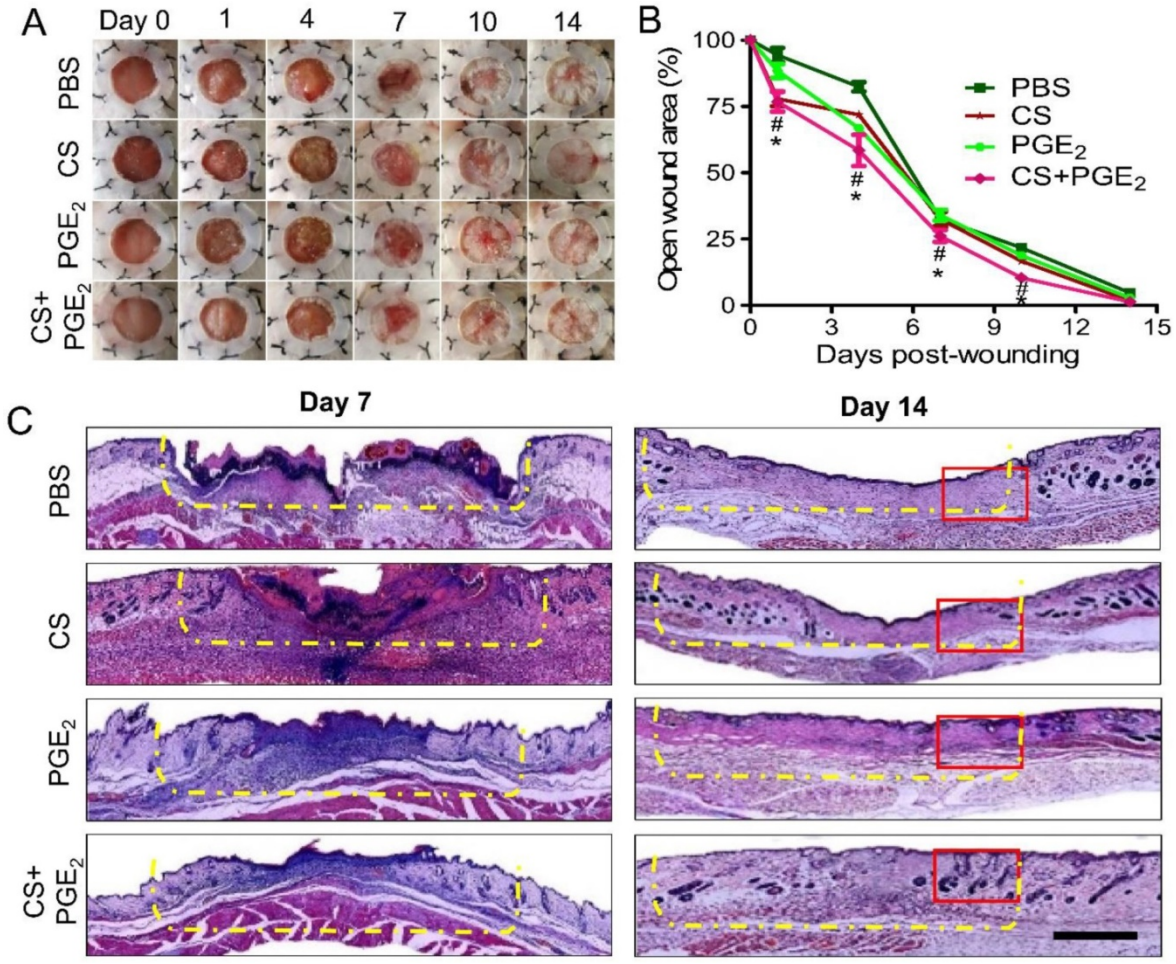


**Figure 2. CS+PGE$_2$ hydrogel accelerated wound healing. (A)** The injury areas were measured every 3 days after treatment. Quantitative analysis of the data revealed that CS+PGE$_2$ hydrogel could improve wound healing. **(B)** The percentage of wound area compared to the original area from day 0 to 14. Data are expressed as mean ± SD. n=10. $^{*}P < 0.05$ versus PBS; $^{\#}P < 0.05$ versus CS. **(C)** Representative images of HE staining at day 14 after treatment with CS+PGE$_2$ hydrogel when the wound was completely closed. The injured sites are indicated by the yellow dashed line. The magnification of the red rectangle is presented in **Figure S1**. Scale bars, 100 μm. CS+PGE$_2$: CS+PGE$_2$ hydrogel; PGE$_2$: free PGE$_2$; CS: chitosan hydrogel; PBS: untreated wounds.

## M2 polarization of macrophages at injured sites

We next explored the distribution of macrophages at the CS+PGE$_2$ hydrogel treatment sites by analyzing recruitment of CD68 and CD206, which are pan-macrophage and M2 macrophage markers respectively [29-31]. CS+PGE$_2$ hydrogel treatment led to a time-dependent increase in the number of CD68 and CD206-positive macrophages (**Figure 5A-B** and **Figure S5**). Next, Western blot analysis revealed that CS+PGE$_2$ hydrogel significantly improved secretion of IL-10, an M2 macrophage-associated molecule. However, CS+PGE$_2$ hydrogel remarkably reduced secretion of IL-6 (**Figure 5C** and **Figure S6**), a pro-inflammatory cytokine. Moreover, the presence of M2 macrophages at the injured sites on day 4 was further confirmed by using specific antibodies to F4/80 and RELM-α, markers of M2 macrophages. CS+PGE$_2$ hydrogel treatment increased accumulation of F4/80- and RELM-α positive cells (**Figure 5D**). These results indicated that CS+PGE$_2$ hydrogel could promote polarization of M2 macrophages at the injured site.

## Enhanced angiogenic effects of CS+PGE$_2$ hydrogel

Angiogenesis is a fundamental process for growth and tissue repair at the site of injury during the early stages of wound healing. To investigate whether CS+PGE$_2$ hydrogel promotes angiogenesis at the sites of injury, *VEGFR2-Luc* transgenic mice were used to establish an excisional skin wound. At different time points after injury, angiogenesis was monitored by BLI in real-time. BLI signal could be detected in all groups, suggesting the feasibility of using BLI to monitor angiogenesis after injury. The strongest signal intensity was observed in the CS+PGE$_2$ hydrogel treatment group, which indicated that CS+PGE$_2$ hydrogel could promote angiogenesis by stimulating VEGF-R2 expression (**Figure 6A-B**). Microvascular density was also significantly

increased by application of CS+$PGE_2$ hydrogel as revealed by CD31 staining, which was consistent with BLI results (**Figure S7A-B**). Furthermore, the expression of proangiogenic genes at the injured sites on day 4 was analyzed, and the results revealed that CS+$PGE_2$ hydrogel treatment remarkably increased the expression of angiogenesis-related genes PLGF, VEGF-A, b-FGF, PDGF-BB, Ang-1, and Ang-2 (**Figure S7C**). These results indicated that CS+$PGE_2$ hydrogel could enhance proangiogenic effects during wound healing.

Numerous studies have shown that macrophages are involved in the regulation of angiogenesis during tissue repair [32-36]. To investigate the proangiogenic effects of CS+$PGE_2$ hydrogel at injured sites, immunostaining was performed by staining of CD206 and CD31 on day 4. The results revealed that a large number of CD206-positive cells gathered around the CD31-positive cells at injured sites (**Figure 6C**).

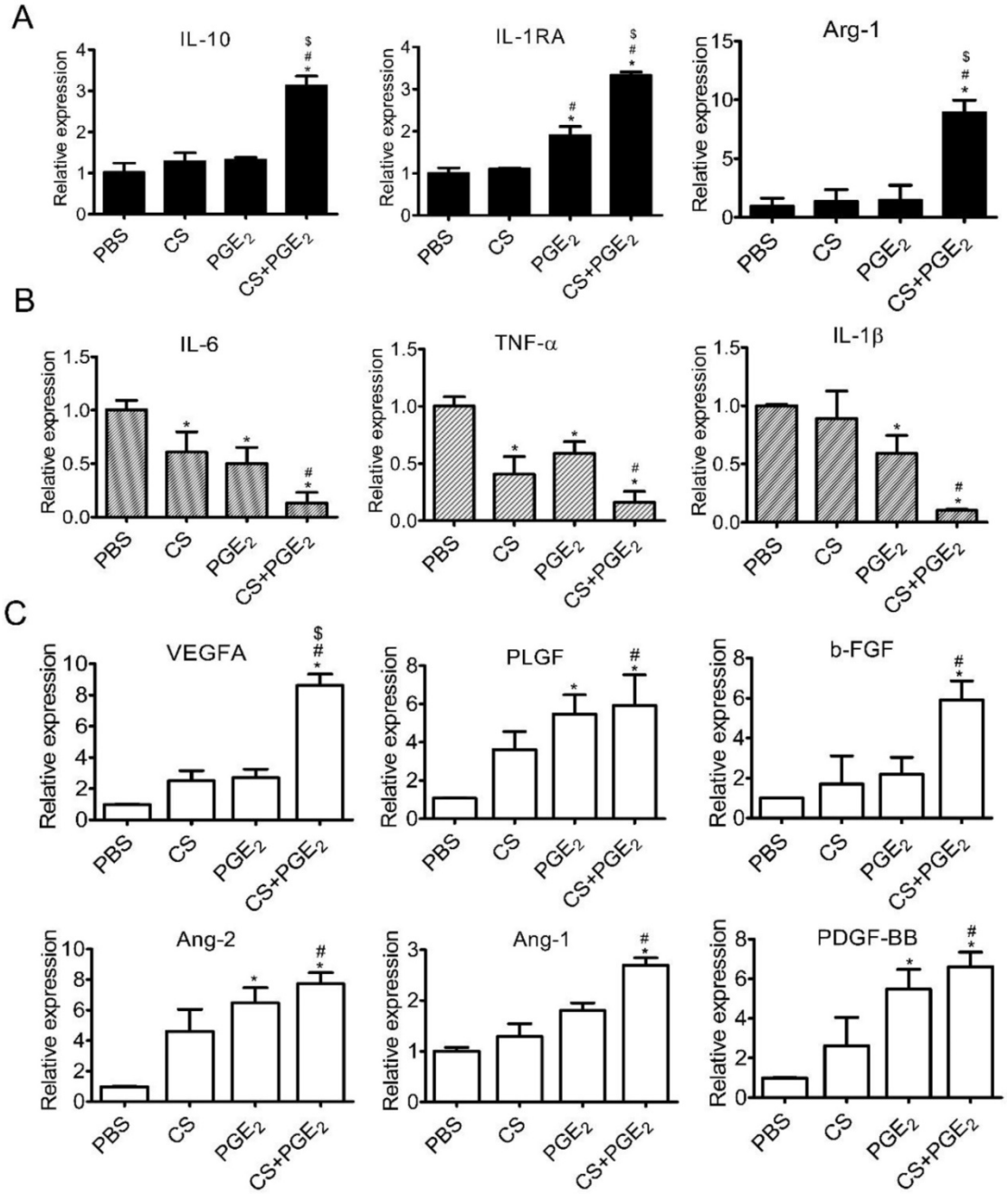


**Figure 3. CS+$PGE_2$ hydrogel enhanced anti-inflammatory and angiogenic effects *in vitro*. (A)** RT-PCR analysis of M2-related gene (IL-10, IL-1Rα, and Arg-1) expression in macrophages. **(B)** RT-PCR analysis of M1-related gene (IL-6, TNF-α, and IL-1β) expression in macrophages. **(D)** RT-PCR analysis of angiogenic factors expressions in macrophages cultured with PBS, CS, $PGE_2$, and CS+$PGE_2$ hydrogel for 48 h. Data are expressed as mean ± SD. **P* < 0.05 versus PBS; #*P* < 0.05 versus CS; $*P* < 0.05 versus $PGE_2$.

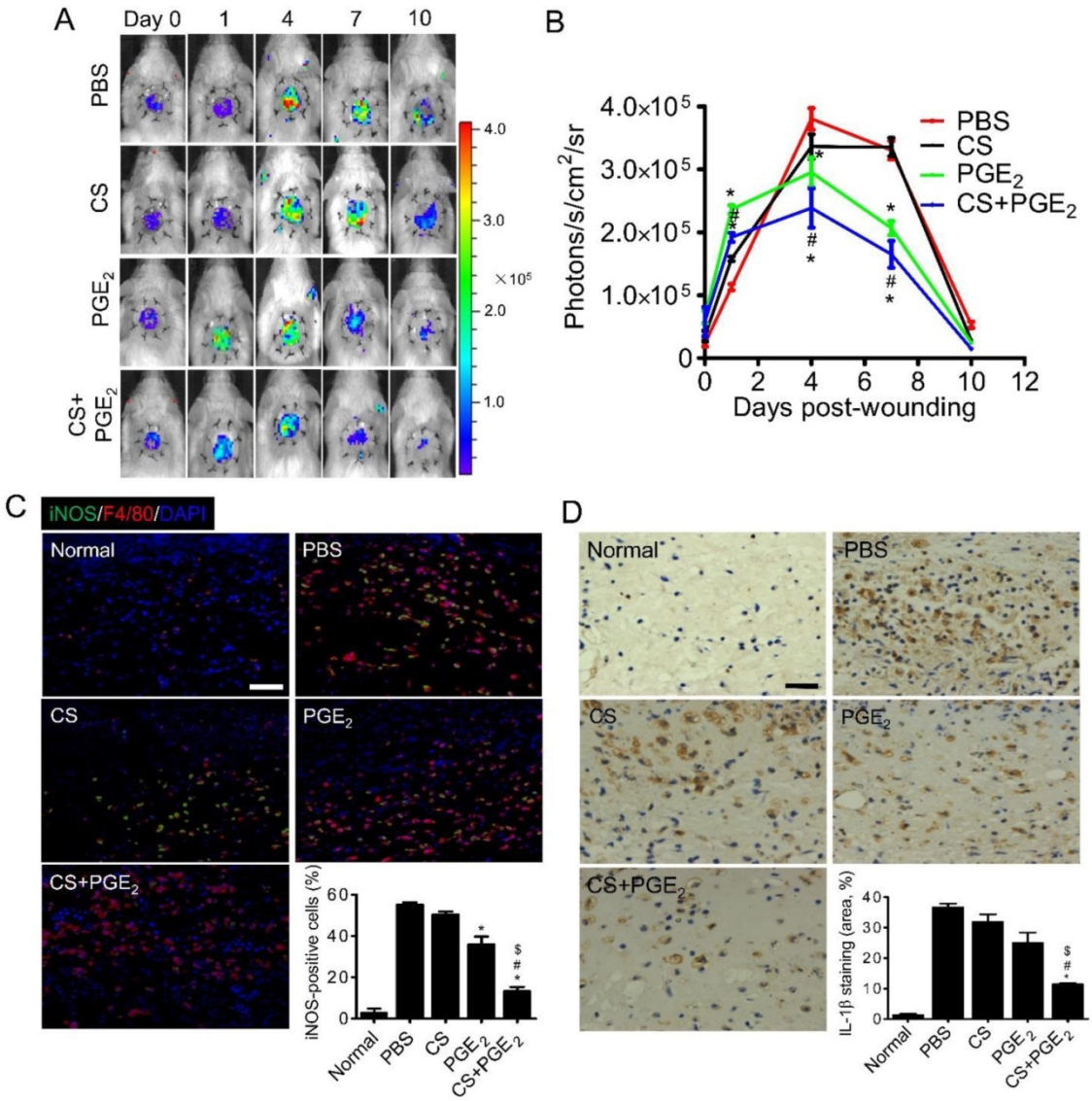


**Figure 4. CS+PGE$_2$ hydrogel enhanced anti-inflammatory effects *in vivo*. (A)** BLI could track ROS activities at the injured sites. **(B)** Quantitative analysis of BLI signals demonstrated that CS+PGE$_2$ hydrogel significantly inhibited ROS at the injured sites. n=8. **(C)** Representative images of iNOS (green) and F4/80 (red) immunostaining showed accumulation of M1 macrophages at the injured sites on day 4. Quantitative analysis revealed that CS+PGE$_2$ hydrogel could reduce accumulation of M1 macrophages. **(D)** Representative images of IL-1β expression at injured sites at day 4. Quantitative analysis revealed that CS+PGE$_2$ hydrogel could inhibit the expression of IL-1β significantly. Data are expressed as mean ± SD. $^*P < 0.05$ versus PBS; $^\#P < 0.05$ versus CS; $^\$P < 0.05$ versus PGE$_2$. Scale bars, 50 μm. CS+PGE$_2$: CS+PGE$_2$ hydrogel; PGE$_2$: free PGE$_2$; CS: chitosan hydrogel; PBS: untreated wounds; Normal: unwounded skin tissue.

## CS+PGE$_2$ hydrogel attenuates skin fibrosis after injury

Wound healing can lead to skin fibrosis resulting in scar formation and ultimately in the loss of skin functions [37] characterized by excessive accumulation of extracellular matrix consisting of mainly collagen I and fibronectin [38]. Thus, the expressions of anti-fibrotic genes including BMP-7 (bone morphogenetic protein-7) and TIMP (tissue inhibitor of metalloproteinase)-1 and -2 were analyzed on day 5 after skin injury. As displayed in **Figure S8**, compared with other groups, CS+PGE$_2$ hydrogel remarkably increased the expression of anti-fibrotic genes, implying that CS+PGE$_2$ hydrogel could exert anti-fibrotic effects during the early stage of skin wound repair. During the development of skin fibrosis, differentiated myofibroblasts are the main cells that produce ECM. Therefore, on day 14 after injury, we performed α-SMA immunofluorescent staining to evaluate infiltration of myofibroblasts in the skin tissue. The results showed that CS+PGE$_2$ hydrogel treatment remarkably decreased the expression of α-SMA (**Figure 7A-B**). Furthermore, Masson trichrome staining showed that CS+PGE$_2$ hydrogel and PGE$_2$ could both decrease the deposition of collagen with the minimum collagen deposition in the CS+PGE$_2$ hydrogel group (**Figure 7C-D**). RT-PCR analysis revealed that collagen type 1α1 (Col1A1), TGF-β, and fibronectin genes were

highly expressed in the PBS group, whereas the expression levels of these genes were significantly reduced in CS or $PGE_2$ treatment groups, especially in the CS+$PGE_2$ hydrogel group (**Figure 7E**). Western blot analysis also suggested that CS+$PGE_2$ hydrogel could significantly reduce the expression of collagen I (**Figure 7F-G**).

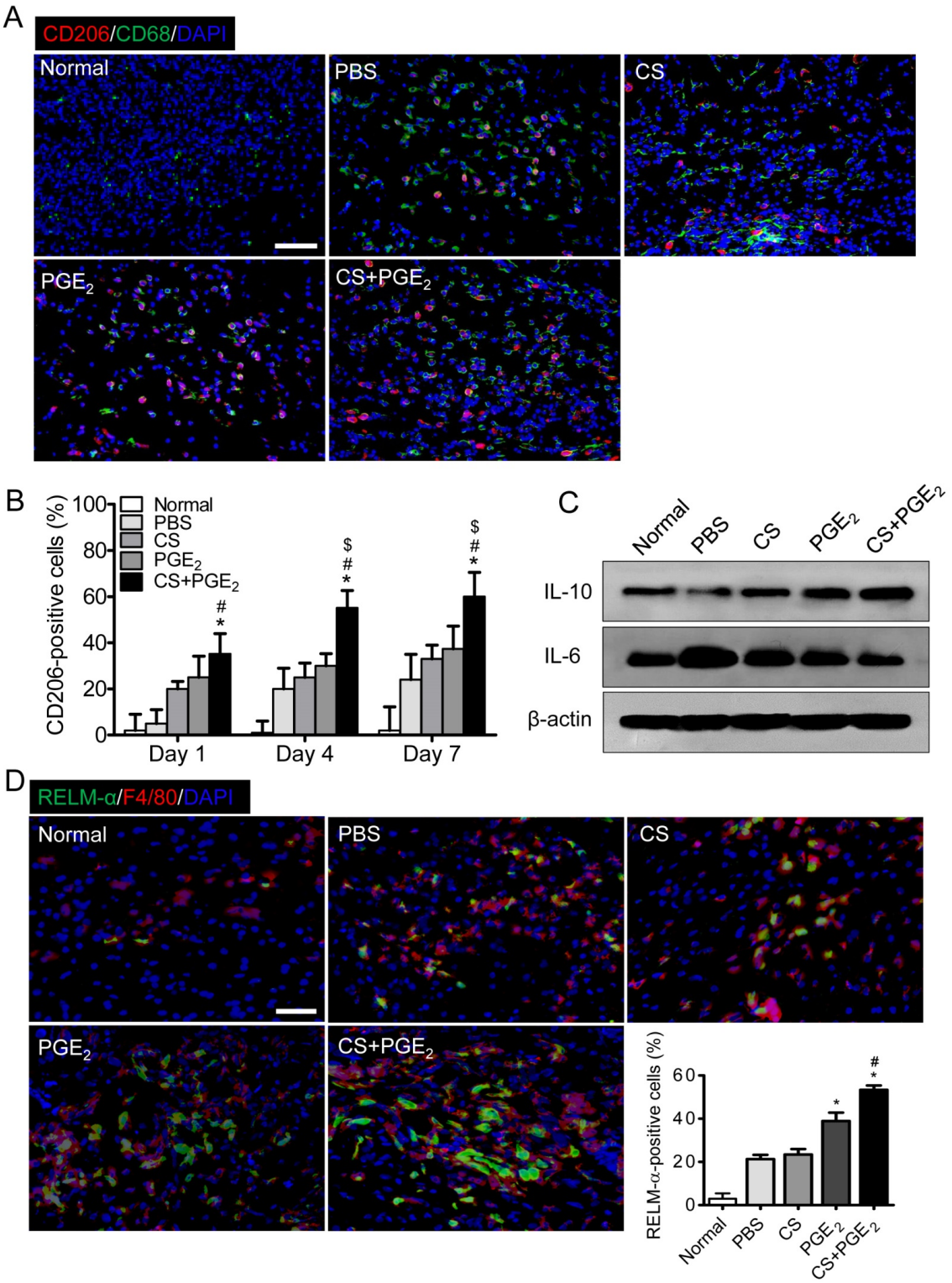


**Figure 5. CS+$PGE_2$ hydrogel promoted polarization of M2 macrophages at injured sites. (A)** Representative images display the expression of M2 and pan-macrophage markers CD206 and CD68 on day 4 at the injured sites. **(B)** Quantitative analysis revealed that CS+$PGE_2$ hydrogel could promote M2 macrophage polarization. n=6. **(C)** Western blot analysis of IL-10 and IL-6 in injured tissues on day 4. **(D)** Representative images of F4/80 (red) and RELM-α (green) expression at injured sites on day 4. Quantitative analysis revealed that CS+$PGE_2$ hydrogel could promote the expression of F4/80 and RELM-α significantly. Data are expressed as mean ± SD. n=6. $^{*}P < 0.05$ versus PBS; $^{\#}P < 0.05$ versus CS. Scale bars, 50 μm. CS+$PGE_2$: CS+$PGE_2$ hydrogel; $PGE_2$: free $PGE_2$; CS: chitosan hydrogel; PBS: untreated wounds; Normal: unwounded skin tissue.

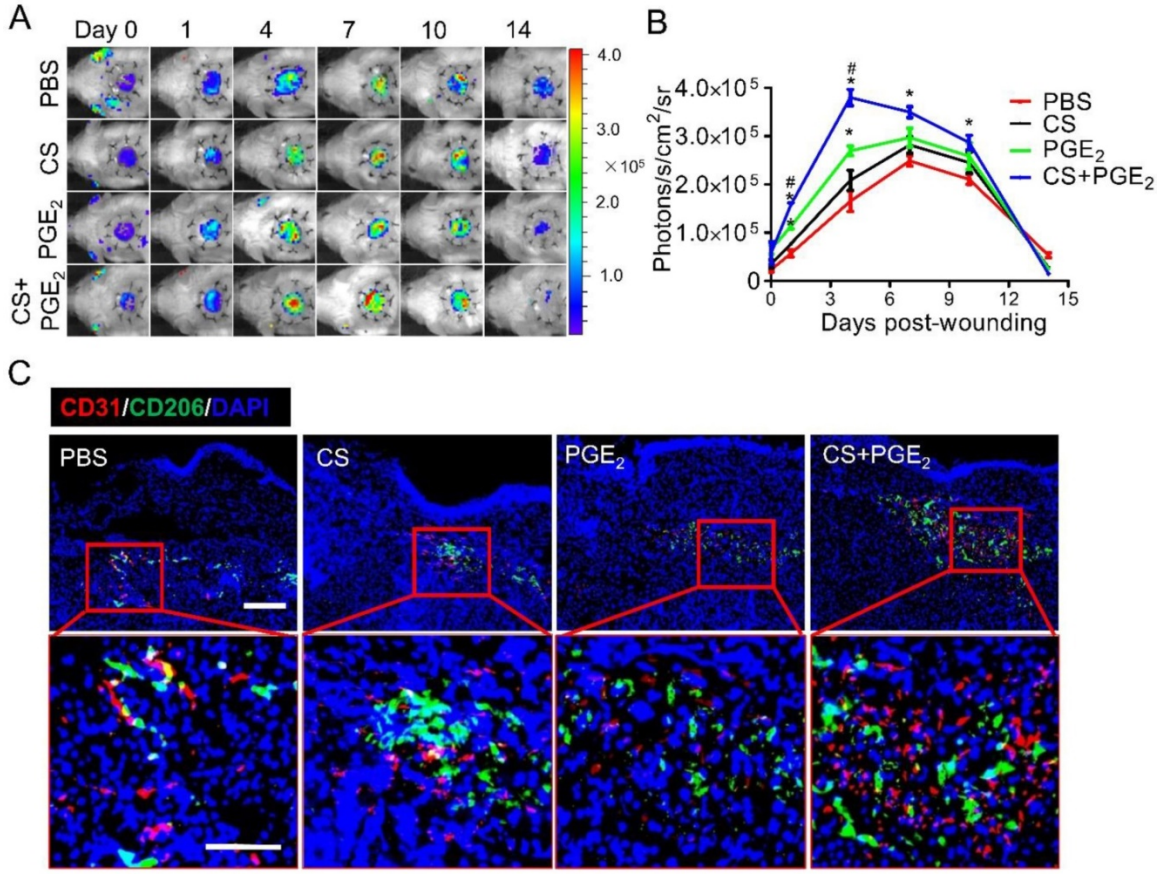


**Figure 6. CS+PGE$_2$ hydrogel enhanced early angiogenesis at injured sites. (A)** Spatiotemporal kinetics of expression of VEGF-R2 was tracked by BLI following CS+PGE$_2$ treatment. **(B)** Quantitative analysis of BLI signals demonstrated that CS+PGE$_2$ hydrogel could promote angiogenesis significantly during the early few days after injury. **(C)** Representative images showed M2 macrophages (CD206, green) and endothelial cells (CD31, red) by double staining on day 4. Scale bars, 50 μm. CS+PGE$_2$: CS+PGE$_2$ hydrogel; PGE$_2$: free PGE$_2$; CS: chitosan hydrogel; PBS: untreated wounds.

## Discussion

In this study, we have shown that CS hydrogel could prolong the release of PGE$_2$ and further enhance its wound healing potential. We further investigated the therapeutic mechanisms of CS+PGE$_2$ hydrogel and determined that prolonged release of PGE$_2$ could direct macrophages to anti-inflammatory, tissue-regenerating, and anti-fibrotic phenotypes. CS+PGE$_2$ hydrogel could regulate the wound microenvironment by inducing M2 polarization of macrophages and could achieve a balance among the three overlapping phases—inflammation, regeneration (angiogenesis), and remodeling (fibrosis)—of cutaneous wound healing (**Figure 7H**). Furthermore, the anti-inflammatory and accelerated cutaneous wound healing effects of CS+PGE$_2$ hydrogel were monitored by molecular imaging in real time.

While the inflammatory response during the first phase of cutaneous wound healing is crucial to protect the organism from infection and further harm, it is also a major factor in the pathogenesis of scar formation [39]. A delicate balance between cytokines and other mediators involved in the inflammatory response of tissue repair is important for optimal therapy in clinical applications. Identifying the dynamic nature of the wound microenvironment and signaling pathways in tissue repair and regeneration would certainly promote treatment of injury and degenerative diseases. In our present study, treatment with CS+PGE$_2$ hydrogel accelerated wound healing while also alleviating fibrosis of the skin tissue after injury. However, multiple dosing of CS+PGE$_2$ hydrogel could lead to tissue hyperplasia, formation of a scar, and even loss of skin functions, suggesting that it is crucial to precisely maintain a dynamic balance between wound healing and collagen deposition. With the recent insights into the molecular mechanisms of macrophages in tissue regeneration following injury, it has become feasible to modulate macrophage actions that might optimize healing of damaged tissues [40].

Macrophages perform a desirable function in the developmental processes and provide nutritional support to the tissues in which they live by producing growth factors and other mediators, demonstrating significant homeostatic activity in almost all organ

systems [41]. The functions of macrophages rely on the change of their phenotypes, which is affected by the local microenvironment during wound healing [42]. In this respect, a better understanding of the intrinsic polarization mechanism of macrophages may allow the development of effective therapeutic approaches in regenerative medicine. In the microenvironment of damaged tissues, lipopolysaccharides (LPS) or interferon (IFN)-γ can induce pro-inflammatory macrophages (M1) that contribute to further tissue injury, inflammation, and subsequent fibrosis by upregulating pro-inflammatory cytokines consisting of tumor necrosis factor (TNF)-α, interleukin (IL)-6, inducible nitric oxide synthase (iNOS), IL-1β, or reactive oxygen species (ROS) [43, 44]. Anti-inflammatory factors, IL-4 or IL-10, in post-inflammatory tissues induce anti-inflammatory macrophages (M2), which could mediate tissue repair and regeneration by secreting high levels of anti-inflammatory factors IL-10, IL-1 receptor antagonist (IL-1RA), and arginase (Arg)-1 [44].

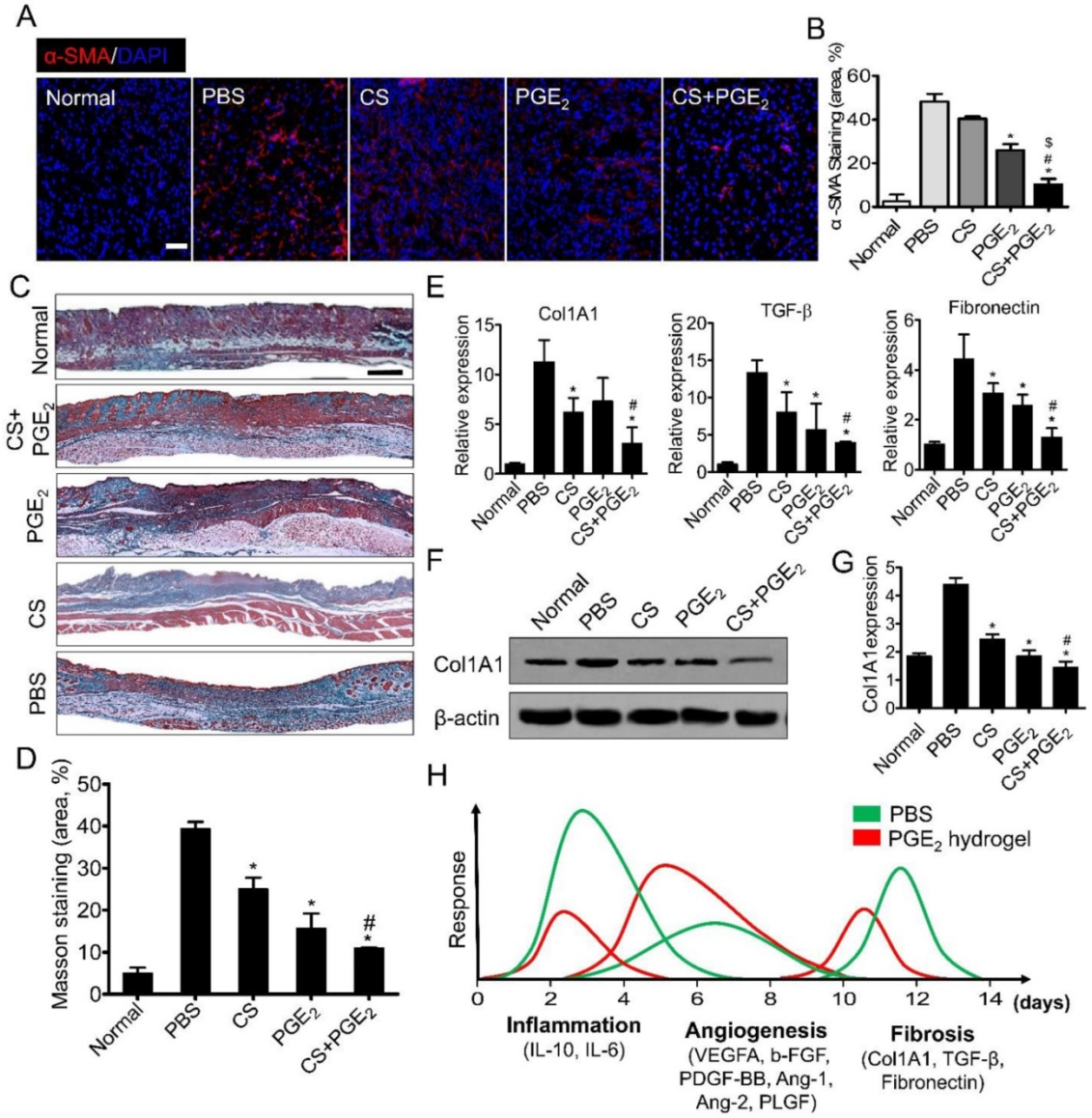


**Figure 7. CS+PGE$_2$ hydrogel treatment attenuated skin fibrosis. (A)** Representative images of α-SMA staining on day 14. **(B)** Quantitative analysis showed that CS+PGE$_2$ hydrogel could reduce the expression of α-SMA significantly. **(C)** Masson trichrome staining showed deposition of collagen on day 14. **(D)** Quantitative analysis revealed that CS+PGE$_2$ hydrogel could decrease deposition of collagen during wound healing. **(E)** Real-time PCR analysis of the expressions of collagen type 1α1, TGF-β, and fibronectin genes on day 14. **(F)** Western blot analysis of the expression of Col1A1 on day 14. **(G)** Quantitative data of the expression of Col1A1. Data are expressed as mean ± SD. *$P$ < 0.05 versus PBS; #$P$ < 0.05 versus CS. All experiments were performed in triplicate. Scale bars, 50 μm. CS+PGE$_2$: CS+PGE$_2$ hydrogel; PGE$_2$: free PGE$_2$; CS: chitosan hydrogel; PBS: untreated wounds; Normal: unwounded skin tissue. **(H)** Schematic diagram depicts the regeneration effects of CS+PGE$_2$ hydrogel. Wound healing events involve different phases including inflammation, tissue regeneration, and remodeling at the injured site. Our results indicated that CS+PGE$_2$ hydrogel could regulate the wound microenvironment by increasing the anti-inflammatory and pro-angiogenic activities of macrophages and alleviating fibrosis. This therapeutic could achieve a balance between the overlapping inflammatory, regenerative (angiogenesis), and remodeling (fibrosis) phases of cutaneous wound healing.

Therapeutics for delivering cytokines, soluble factors, biomaterials, and stem cells targeting macrophages offer the promise to regulate the phenotypic switch of macrophages and then enhance wound healing and regeneration. Tissue repair by MSC-induced M2 macrophages is likely to be attributed to secretion of $PGE_2$ by MSCs [13]. $PGE_2$ could stimulate IL-10 secretion of macrophages or polarization of M2 macrophages, thereby inhibiting secretion of TGF-β and IL-6 and further reducing deposition of collagen [45]. Our study confirmed this effect and demonstrated that CS+$PGE_2$ hydrogel could promote the switch from M1 to M2 phenotype of macrophages in an inflammatory environment and accelerate skin wound healing. This indicated that application of CS+$PGE_2$ hydrogel could exert the desired therapeutic effect. Recent advances in stem cell biology indicate that the paracrine action of MSCs plays an essential role in reparative processes [22, 46]. Characterization of the specific MSC secretome profile including growth factors, cytokines, microRNAs and hormones, will provide a ready-to-use and cell-free therapeutic alternative to cell-based therapy [47].

Synthetic or natural materials serving as drug carriers or scaffolds exhibit great potential in tissue repair and regeneration [24, 48]. Naturally derived biomaterials including agar, agarose, collagen, gelatin, alginate, chitosan, hyaluronic acid, fibrin/fibrinogen, and silk have been widely used for regeneration therapy [49]. Thermosensitive chitosan hydrogel, which can transform from liquid at room temperature to hydrogel at 37 ℃, has been used as a wound dressing for hemostasis in cutaneous wound healing [50]. Engineered matrices with cytokines could sustain the release and improve the local retention of regenerative factors, which are required during tissue regeneration [51]. Chitosan can establish intermolecular interactions between amines and carboxyl groups with linear polysaccharides of N-acetylglucosamine and glucosamine, and can load growth factors, cytokines, and small molecules for controlled release [48, 50]. In addition, the size of the pore structures in CS hydrogel can affect loading and release of $PGE_2$. Future success of clinical applications of CS-$PGE_2$ hydrogel rely on optimization of $PGE_2$ release to regulate the temporal and spatial molecular signals precisely at the injury sites during wound healing.

Wound healing is well regulated by overlapping phases and a complex series of events including inflammation, proliferation, and remodeling. Dysregulation in certain stages of the healing processes results in formation of abnormal scars or chronic non-healing wounds. For example, excessive M1 macrophages lead to chronic inflammation and tissue destruction and excessive M2 macrophages promote fibrosis [1]. Molecular imaging can visualize cellular functions and molecular processes in live animals and can access detailed molecular events at the molecular-pathology level during certain wound healing stages [22, 52]. In this study, we provided dynamic real-time imaging by BLI of ROS and VEGFR2 in the wound healing stages of inflammation and regeneration. During wound healing, angiogenesis provides oxygen to injured sites, thus promoting tissue repair and regeneration. Thus, we can conclude that CS+$PGE_2$ hydrogel can downregulate the inflammatory response and enhance tissue regeneration. By providing insights into the molecular mechanisms governing tissue repair and regeneration, our study highlights the importance of molecular imaging in developing an optimal therapeutic strategy for promoting tissue regeneration [19, 53].

## Conclusion

In summary, we developed and characterized a CS+$PGE_2$ hydrogel for cutaneous wound healing. Incorporation of $PGE_2$ into the CS hydrogel could prolong its release and enhance therapeutic effects for tissue repair and regeneration. CS+$PGE_2$ hydrogel increased anti-inflammatory and angiogenesis-related factors contributing to tissue repair after injury. Increased polarization of M2 macrophages at the site of injury was identified as a novel mechanism to promote tissue damage repair. Moreover, molecular imaging used in this study elucidated the signaling pathways involved in wound healing during inflammation and in the transition to the proliferative phase. Taken together, these findings highlight the potential of CS+$PGE_2$ hydrogel as a novel therapeutic strategy for promoting tissue regeneration.

## Abbreviations

Ang-1: angiopoietin 1; Ang-2: angiopoietin 2; Arg-1: arginase-1; bFGF: basic fibroblast growth factor; BLI: bioluminescence imaging; BMP-7: bone morphogenetic protein-7; CD206: cluster of differentiation 206; CD31: platelet endothelial cell adhesion molecule-1; CD68: cluster of differentiation-68; Col1A1: collagen type 1α1; CS: chitosan; DAPI: 4′, 6-diamidino-2-phenylindole; ECM: extracellular matrix; ELISA: enzyme-linked immunosorbent assay; HE: hematoxylin and eosin; IFN-γ: interferon-γ; IL-10: interleukin-10; IL-1RA: interleukin 1 receptor antagonist; IL-1β: interleukin-β; IL-4: interleukin-4; IL-6: interleukin-6; iNOS: inducible nitric oxide synthase; LPS: lipopolysaccharides; MSCs: mesenchymal stem cells; PDGF-BB: platelet-derived growth factor BB; $PGE_2$: prostaglandin $E_2$; PLGF:

placental growth factor; RELM-α: resistin-like molecule-α; RIPA: radio-immunoprecipitation assay; ROS: reactive oxygen species; SEM: scanning electron microscopy; TGF-β: transforming growth factor-β; TIMP-1: tissue inhibitor of metalloproteinase-1; TIMP-2: tissue inhibitor of metalloproteinase-2; TNF-α: tumor necrosis factor-α; VEGF-A: vascular endothelial growth factor A; VEGF-R2: vascular endothelial growth factor receptor 2; VEGFR2-luc: vascular endothelial growth factor receptor 2-luciferase transgenic mouse.

## Acknowledgments

This research was partially supported by National Key R&D Program of China (2017YFA0103200), National Natural Science Foundation of China (81320108014, 81671734, 31470951), Tianjin Natural Science Foundation (16ZXMJSY00060), Natural Science Foundation of Jiangxi (20161BAB205281), Key Projects of Tianjin Science and Technology Support Program (18YFZCSY00010), and Fundamental Research Funds for the Central Universities (63181114).

## Supplementary Material

Supplementary figures and tables.
http://www.thno.org/v08p5348s1.pdf

## Competing Interests

The authors have declared that no competing interest exists.

## References

1. Spiller KL, Koh TJ. Macrophage-based therapeutic strategies in regenerative medicine. Adv Drug Deliv Rev. 2017; 122: 74-83.
2. Lohmann N, Schirmer L, Atallah P, Wandel E, Ferrer RA, Werner C, et al. Glycosaminoglycan-based hydrogels capture inflammatory chemokines and rescue defective wound healing in mice. Sci Transl Med. 2017; 9: eaai9044.
3. Yoon DS, Lee Y, Ryu HA, Jang Y, Lee K-M, Choi Y, et al. Cell recruiting chemokine-loaded sprayable gelatin hydrogel dressings for diabetic wound healing. Acta Biomater. 2016; 38: 59-68.
4. Forbes SJ, Rosenthal N. Preparing the ground for tissue regeneration: from mechanism to therapy. Nat Med. 2014; 20: 857-69.
5. Wynn TA, Vannella KM. Macrophages in tissue repair, regeneration, and fibrosis. Immunity. 2016; 44: 450-62.
6. Zhang Y, Desai A, Yang SY, Bae KB, Antczak MI, Fink SP, et al. Inhibition of the prostaglandin-degrading enzyme 15-PGDH potentiates tissue regeneration. Science. 2015; 348: aaa2340.
7. Vannella KM, Wynn TA. Mechanisms of organ injury and repair by macrophages. Annu Rev Physiol. 2017; 79: 593-617.
8. Ip WKE, Hoshi N, Shouval DS, Snapper S, Medzhitov R. Anti-inflammatory effect of IL-10 mediated by metabolic reprogramming of macrophages. Science. 2017; 356: 513-9.
9. Patel U, Rajasingh S, Samanta S, Cao T, Dawn B, Rajasingh J. Macrophage polarization in response to epigenetic modifiers during infection and inflammation. Drug Discov Today. 2017; 22: 186-93.
10. Han CZ, Juncadella IJ, Kinchen JM, Buckley MW, Klibanov AL, Dryden K, et al. Macrophages redirect phagocytosis by non-professional phagocytes and influence inflammation. Nature. 2016; 539: 570-4.
11. Chen J, Yang J, Liu R, Qiao C, Lu Z, Shi Y, et al. Dual-targeting theranostic system with mimicking apoptosis to promote myocardial infarction repair via modulation of macrophages. Theranostics. 2017; 7: 4149-67.
12. Nemeth K, Leelahavanichkul A, Yuen PS, Mayer B, Parmelee A, Doi K, et al. Bone marrow stromal cells attenuate sepsis via prostaglandin E(2)-dependent reprogramming of host macrophages to increase their interleukin-10 production. Nat Med. 2009; 15: 42-9.
13. Zhang QZ, Su WR, Shi SH, Wilder-Smith P, Xiang AP, Wong A, et al. Human gingiva-derived mesenchymal stem cells elicit polarization of m2 macrophages and enhance cutaneous wound healing. Stem Cells. 2010; 28: 1856-68.
14. Takeuchi K, Tanigami M, Amagase K, Ochi A, Okuda S, Hatazawa R. Endogenous prostaglandin E2 accelerates healing of indomethacin-induced small intestinal lesions through upregulation of vascular endothelial growth factor expression by activation of EP4 receptors. J Gastroenterol Hepatol. 2010; 25 Suppl 1: S67-74.
15. Takeuchi K. Prophylactic effects of prostaglandin E2 on NSAID-induced enteropathy-role of EP4 receptors in its protective and healing-promoting effects. Curr Opin Pharmacol. 2014; 19: 38-45.
16. Crunkhorn S. Regenerative medicine: Inhibiting prostaglandin breakdown triggers tissue regeneration. Nat Rev Drug Discov. 2015; 14: 526.
17. Duffin R, O'Connor RA, Crittenden S, Forster T, Yu C, Zheng X, et al. Prostaglandin E(2) constrains systemic inflammation through an innate lymphoid cell-IL-22 axis. Science. 2016; 351: 1333-8.
18. Ho ATV, Palla AR, Blake MR, Yucel ND, Wang YX, Magnusson KEG, et al. Prostaglandin E2 is essential for efficacious skeletal muscle stem-cell function, augmenting regeneration and strength. Proc Natl Acad Sci U S A. 2017; 114: 6675-84.
19. Feng G, Zhang J, Li Y, Nie Y, Zhu D, Wang R, et al. IGF-1 C Domain-Modified Hydrogel Enhances Cell Therapy for AKI. J Am Soc Nephrol. 2016; 27: 2357-69.
20. Xu Q, Guo L, Sigen A, Gao Y, Zhou D, Greiser U, et al. Injectable hyperbranched poly (β-amino ester) hydrogels with on-demand degradation profiles to match wound healing processes. Chem Sci. 2018; 9: 2179-87.
21. Danon D, Kowatch MA, Roth GS. Promotion of wound repair in old mice by local injection of macrophages. Proc Natl Acad Sci U S A. 1989; 86: 2018-20.
22. Du W, Zhang K, Zhang S, Wang R, Nie Y, Tao H, et al. Enhanced proangiogenic potential of mesenchymal stem cell-derived exosomes stimulated by a nitric oxide releasing polymer. Biomaterials. 2017; 133: 70-81.
23. Galiano RD, Michaels Jt, Dobryansky M, Levine JP, Gurtner GC. Quantitative and reproducible murine model of excisional wound healing. Wound Repair Regen. 2004; 12: 485-92.
24. Zhang K, Zhao X, Chen X, Wei Y, Du W, Wang Y, et al. Enhanced therapeutic effects of MSC-derived exosomes with an injectable hydrogel for hindlimb ischemia treatment. ACS Appl Mater Interfaces. 2018; 10: 30081-91.
25. Mao D, Zhu M, Zhang X, Ma R, Yang X, Ke T, et al. A macroporous heparin-releasing silk fibroin scaffold improves islet transplantation outcome by promoting islet revascularisation and survival. Acta Biomater. 2017; 59: 210-20.
26. Koh TJ, DiPietro LA. Inflammation and wound healing: the role of the macrophage. Expert Rev Mol Med. 2011; 13: e23.
27. Kim H, Kim Y, Kim IH, Kim K, Choi Y. ROS-responsive activatable photosensitizing agent for imaging and photodynamic therapy of activated macrophages. Theranostics. 2013; 4: 1-11.
28. Chen WT, Tung CH, Weissleder R. Imaging reactive oxygen species in arthritis. Mol Imaging. 2004; 3: 159-62.
29. Ben-Mordechai T, Holbova R, Landa-Rouben N, Harel-Adar T, Feinberg MS, Abd Elrahman I, et al. Macrophage subpopulations are essential for infarct repair with and without stem cell therapy. J Am Coll Cardiol. 2013; 62: 1890-901.
30. Patel SK, Janjic JM. Macrophage targeted theranostics as personalized nanomedicine strategies for inflammatory diseases. Theranostics. 2015; 5: 150-72.
31. Zhang C, Yu X, Gao L, Zhao Y, Lai J, Lu D, et al. Noninvasive imaging of CD206-positive M2 macrophages as an early biomarker for post-chemotherapy tumor relapse and lymph node metastasis. Theranostics. 2017; 7: 4276-88.
32. Willenborg S, Lucas T, van Loo G, Knipper JA, Krieg T, Haase I, et al. CCR2 recruits an inflammatory macrophage subpopulation critical for angiogenesis in tissue repair. Blood. 2012; 120: 613-25.
33. Pollard JW. Trophic macrophages in development and disease. Nat Rev Immunol. 2009; 9: 259-70.
34. Gordon S, Taylor PR. Monocyte and macrophage heterogeneity. Nat Rev Immunol. 2005; 5: 953-64.
35. Lingen MW. Role of leukocytes and endothelial cells in the development of angiogenesis in inflammation and wound healing. Arch Pathol Lab Med. 2001; 125: 67-71.
36. Bergmann CE, Hoefer IE, Meder B, Roth H, van Royen N, Breit SM, et al. Arteriogenesis depends on circulating monocytes and macrophage accumulation and is severely depressed in op/op mice. J Leukoc Biol. 2006; 80: 59-65.
37. Eming SA, Martin P, Tomic-Canic M. Wound repair and regeneration: mechanisms, signaling, and translation. Sci Transl Med. 2014; 6: 265sr6.
38. Ray S, Ju X, Sun H, Finnerty CC, Herndon DN, Brasier AR. The IL-6 trans-signaling-STAT3 pathway mediates ECM and cellular proliferation in fibroblasts from hypertrophic scar. J Invest Dermatol. 2013; 133: 1212-20.
39. Braga TT, Agudelo JS, Camara NO. Macrophages during the fibrotic process: M2 as friend and foe. Front Immunol. 2015; 6: 602.
40. Courties G, Heidt T, Sebas M, Iwamoto Y, Jeon D, Truelove J, et al. In vivo silencing of the transcription factor IRF5 reprograms the macrophage phenotype and improves infarct healing. J Am Coll Cardiol. 2014; 63: 1556-66.

41. Wynn TA, Chawla A, Pollard JW. Macrophage biology in development, homeostasis and disease. Nature. 2013; 496: 445-55.
42. Murray PJ, Wynn TA. Protective and pathogenic functions of macrophage subsets. Nat Rev Immunol. 2011; 11: 723-37.
43. Lee S, Huen S, Nishio H, Nishio S, Lee HK, Choi BS, et al. Distinct macrophage phenotypes contribute to kidney injury and repair. J Am Soc Nephrol. 2011; 22: 317-26.
44. Lucas T, Waisman A, Ranjan R, Roes J, Krieg T, Muller W, et al. Differential roles of macrophages in diverse phases of skin repair. J Immunol. 2010; 184: 3964-77.
45. Liechty KW, Kim HB, Adzick NS, Crombleholme TM. Fetal wound repair results in scar formation in interleukin-10-deficient mice in a syngeneic murine model of scarless fetal wound repair. J Pediatr Surg. 2000; 35: 866-72.
46. Hassan WU, Greiser U, Wang W. Role of adipose-derived stem cells in wound healing. Wound Repair Regen. 2014; 22: 313-25.
47. Monsanto MM, Wang BJ, Sussman MA. Synthetic MSC? Nothing beats the real thing. Circ Res. 2017; 120: 1694-5.
48. Cui Z, Yang B, Li R-K. Application of biomaterials in cardiac repair and regeneration. Engineering. 2016; 2: 141-8.
49. Choudhury D, Tun HW, Wang T, Naing MW. Organ-derived decellularized extracellular matrix: a game changer for bioink manufacturing? Trends Biotechnol. 2018; 36: 787-805.
50. Zhao X, Wu H, Guo B, Dong R, Qiu Y, Ma PX. Antibacterial anti-oxidant electroactive injectable hydrogel as self-healing wound dressing with hemostasis and adhesiveness for cutaneous wound healing. Biomaterials. 2017; 122: 34-47.
51. He N, Xu Y, Du W, Qi X, Liang L, Wang Y, et al. Extracellular matrix can recover the downregulation of adhesion molecules after cell detachment and enhance endothelial cell engraftment. Sci Rep. 2015; 5: 10902.
52. He N, Chen X, Wang D, Xu K, Wu L, Liu Y, et al. VE-Cadherin regulates the self-renewal of mouse embryonic stem cells via LIF/Stat3 signaling pathway. Biomaterials. 2018; 158: 34-43.
53. Du W, Tao H, Zhao S, He ZX, Li Z. Translational applications of molecular imaging in cardiovascular disease and stem cell therapy. Biochimie. 2015; 116: 43-51.